

We are IntechOpen, the world's leading publisher of Open Access books Built by scientists, for scientists

4,800

Open access books available

122,000

International authors and editors

135M

Downloads

Our authors are among the

154

Countries delivered to

TOP 1%

most cited scientists

12.2%

Contributors from top 500 universities



WEB OF SCIENCE™

Selection of our books indexed in the Book Citation Index
in Web of Science™ Core Collection (BKCI)

Interested in publishing with us?
Contact book.department@intechopen.com

Numbers displayed above are based on latest data collected.

For more information visit www.intechopen.com



Burst and Leak Behaviour of SCC Degraded SG Tubes of PWRs

Seong Sik Hwang, Man Kyo Jung, Hong Pyo Kim and Jung Soo Kim
*Korea Atomic Energy Research Institute
Republic of Korea*

1. Introduction

Steam generators of Pressurized Water Reactor (PWR) have suffered from many types of corrosion, such as pitting, wastage and stress corrosion cracking (SCC) in the primary and secondary sides (Kim 2003, MacDonald, 1996). Some failure events of steam generator tube have been reported in some nuclear power plants around the world (MacDonald, 1996). In order to prevent the primary coolant from leaking into the secondary side, the tubes are repaired by sleeving or plugging (Benson, 1999). It is important to establish the repair criteria to maintain the plugging ratio within a plugging limit which allows successful plant operation.

In the international steam generator tube integrity program (ISG TIP) supported by the US NRC (Nuclear Regulatory Commission), tasks such as in-service inspection technology development, and studies on steam generator tube degradation modes had been undertaken. As a part of the cooperation work, leak and burst tests were carried out, and the burst behaviour of axial mechanical flaws was studied. Leak rate from archive tubes were measured under different water pressures in order to understand the leak behaviour under operating and accident conditions of PWRs.

2. Experimental

2.1 Burst pressure measurement of mechanical notched specimens

Various types of axial (longitudinal along the tube) EDM notches were machined on SG tubes of 195 mm long. The tubes were 19.05 mm in outside diameter, and 1.07 mm in thickness as shown in Table 1. They were fabricated from high temperature mill annealed alloy 600, of which the yield strength and ultimate tensile strength were 241 MPa and 655 MPa, respectively. The leak rate and ligament rupture pressure for the part through-wall defects were measured for the tubes at room temperature. The lengths of the part through-wall defects ranged from 5 mm to 62 mm.

Tests with 100 % axial through-wall defects were carried out to measure tube burst pressure at room temperature. The lengths of the 100% through-wall defects ranged from 12 mm to 30 mm. A flexible plastic tube is usually used for the through-wall defect to ensure leak tightness during the pressurization (Cochet, 1991). In this test, however, it was attempted to obtain crack opening displacement (COD) variation during a slow pressurization. Flexible

Tygon™ tubes (bladder) of 175 mm long were used for 100% through-wall tubes in both slow pressurization and fast pressurization.

Number of tests	Tube Dimension, mm	Flaw type	Flaw length, mm	Flaw depth % TW*	Bladder
33	19.05 OD x 1.07 t	EDM notch Axial	5-62	50, 60, 75, 80, 100	With or Without

% TW*: % tube wall penetration depth

Table 1. Information on the tested tubes

To determine the impact of the pressurization rate on the rupture/ burst pressure, different pressurization rates were applied for the same types of tube defects. Water leak rates just after the ligament rupture or burst were measured by a balance; water coming out of the failed tube was collected in a plastic container for designated time, and the leak rate was calculated by dividing the amount of water by time. The water flow rate through the tubes and the pressures versus time were recorded on a computer. Evolutions of the crack opening during the pressurization were recorded using a conventional digital camera.

The length and depth of the defects of the tubes were measured using eddy current, and the tubes were transferred to the leak and pressure test.

Table

Leak rate tests were performed for the degraded tubes specimens at room-temperature using a high pressure leak-rupture test facility (Fig. 1).

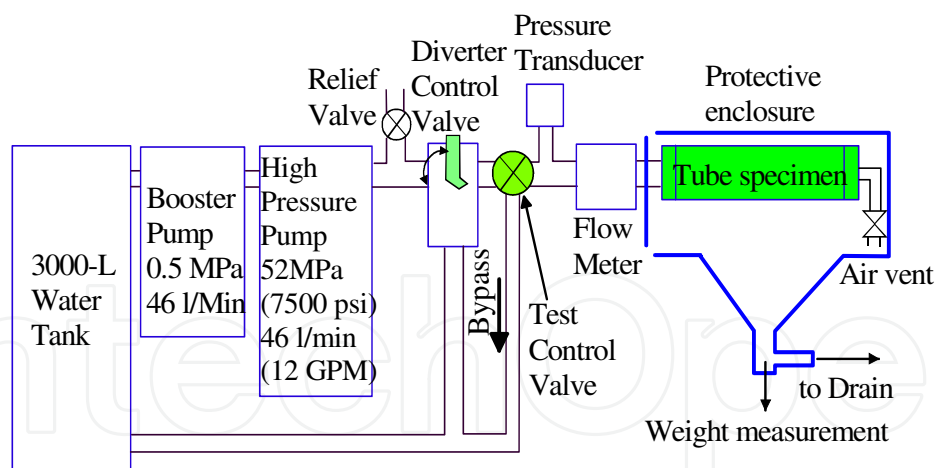


Fig. 1. High pressure leak and burst test facility

2.2 Development of SCC tubes

Laboratory induced stress corrosion cracks were developed in steam generator tube specimens using the ANL SCC production facility and the techniques described in reference (Diercks 2000). Two heats of Korean archive alloy 600 tubes (Heat NX 9824, NX 6312, Carbon 0.024 %) were used in the work. The alloy 600 tubings, which have a 19.05 mm outer diameter and a 1.07 mm wall thickness, are mill annealed at high temperature. The tube specimens, which are 356 mm long, were sensitized at 600 °C for 48 hours in a vacuum tube

furnace. In order to avoid any oxidation on the surface of the tubes, the furnace was vacuumed and back filled with helium and hydrogen gas mixture three times. The surface of the tubes was abraded by emery paper # 600 followed by acetone cleaning before being subjected to the SCC development.

The outside diameters (OD) of the tube specimens were exposed to 1 M sodium tetrathionate solution at room temperature and pressurized with nitrogen gas to a pressure of 20.7 MPa. The cracking procedure was stopped when a pressure drop on the tube was observed, indicating that a leak had occurred. The time to form the through wall crack varied from 69 hours to 607 hours depending on the tube. Crack development test conditions and results for each tube are shown in Table 2. The length and depth of the defects of the tubes were checked by the eddy current method, and the tubes were transferred to the leak and pressure test step.

Tube ID	Crack type	SCC Time(hours)	Cursory ECT
SGH001	OD axial	68.8	OD, 95%/5.08mm, 90%/11.43mm
SGH002	"	67.8	Axial indication(1)
SGH005	"	68.8	90%/15.2mm
SGH006	"	68.8	Axial indication(1)
SGH009	"	404	OD, 80%/10.2mm
SGH010	"	607	OD, 85%.5.08mm
SGH012	ID axial	264	ID, 100%. 24mm

(1) Not quantified

-Material: Alloy 600 HTMA ->Sensitized for 48 hrs @ 600 °C

-SCC developed in 1 M Na₂S₄O₆ at Room Temp.

Table 2. Laboratory Stress Corrosion Cracking of the Archive Tubes

2.3 Large leak rate measurement

Leak rates in the degraded tubes were measured in a room-temperature, high-pressure test facility and a high-temperature, pressure test facility. The room temperature test facility is equipped with a water pressurizing pump, a test specimen section, a control unit and is described in NUREG/ CR-6511 (Diercks 1998). In this facility, the first leak from the tube can be detected by eye through the transparent plastic window, and the leak rate at a given pressure can be measured by weighing the water from the leak. The pressure was held at 10.8, 13.8, 17.2, 20.7 and 27.6 MPa for 5 to 10 minutes to determine the variation of the leak rate with the pressure. For some tubes, the burst pressures were determined.

A high temperature pressure test was undertaken to investigate the leak behaviour at the PWR operating temperature of 282 °C. The high-temperature facility consists of a high temperature water reservoir and a test section where the temperature of the specimen and the pressure difference across the tube are controlled. The maximum pressure difference in this test is around 19.3 MPa. Details of this facility are also described in NUREG CR-6511 (Diercks 1998).

During the first stage of the room temperature pressure testing, the pressure at the first leak, the leak rate at certain pressures and the burst pressures were determined. Two specimens,

SGH002 and SGH006, were prepared for this work. In the second stage of the test, 0.7 MPa pressure increments and 4 to 10 minute holds were adapted to obtain the first leak pressure and leak rate changes with time. The pressurization was stopped when a measurable leak rate could be obtained to avoid an unstable burst, which makes the metallography harder. Specimens SGH001, SGH005, SGH009, and SGH010 were used for this analysis.

For the high temperature pressure test, specimens SGH005 and SGH012 were used. The pressure was raised to 8.3 MPa and held for 45 minutes and then increased to 19.0 MPa slowly while checking for an indication of a leak at the muffler at the exit of the test section.

2.4 Time dependent leak rate measurement

The inside of the tube was pressurized with water. The water pressure was increased until the tube shows a leakage. The first leak from the tube can be detected visually by the naked eye through a transparent plastic window. The leak rate at a given pressure was measured by weighing the water from the leak. The pressure was held at a certain value for a designated time to measure a leak rate. The water pressure was then increased further while opening the crack. The pressurization was stopped when no increase of the leak rate was recorded. Leak rates were measured under constant pressures at different elapsed times in order to observe a change of the leak rate with time.

2.5 Leak rate prediction method

Leak rate based on the prediction model developed by ANL was adapted in order to analyse the leak behaviour of the archive tubes (Majumdar 2000). The equation used in the analysis is:

$$Q = 50.9 \times 10^6 A (P/\rho)^{0.5} \text{ [l/ min]} \quad (1)$$

Where A is the crack opening area in m², P is the pressure difference across the tube wall in MPa, and ρ is the density of the water in kg/ m³ (1000 kg/ m³ at room temperature, 735 kg/ m³ at 282 °C). Fracture mechanics analyses were done to calculate the crack opening area, using the methods described in Refs (Majumdar 2000, Zahoor 1989). In the case of the Korean tubes that had been heat-treated as part of the process for producing SCC, the yield stress was considered to be the same as the received materials based on a prior experience with heat treatment. Yield stress for a high temperature calculation was estimated to be 10% lower than that at the room temperature (Majumdar 2000). Yield stress of 265.5 MPa and 248.2 MPa for UC4 and YG5,6 respectively was used for the room temperature evaluation. In the case of a high temperature calculation for SGH005, 221.3 MPa was used as the reduced yield stress in the leak rate calculation at 282 °C.

3. Results and discussion

3.1 Crack opening displacement of axial notches

COD as a function of the applied pressure is important in the modeling of a ligament rupture or the burst pressure in SG tubes. In the preliminary test, the COD increased a little as the pressure increased during the slow pressurization as shown in Fig. 2. When the pressure reached 10 MPa, the flaw began to show a COD increase. The COD corresponding to an applied pressure of 36 MPa was larger than that corresponding to 10 MPa. Whereas the tube integrity was sustained before ligament rupture, a small pressure increase of 1 MPa

caused the tube ligament rupture followed by a burst. Finally, the tube showed a fish-mouth like opening as shown in Fig. 2.

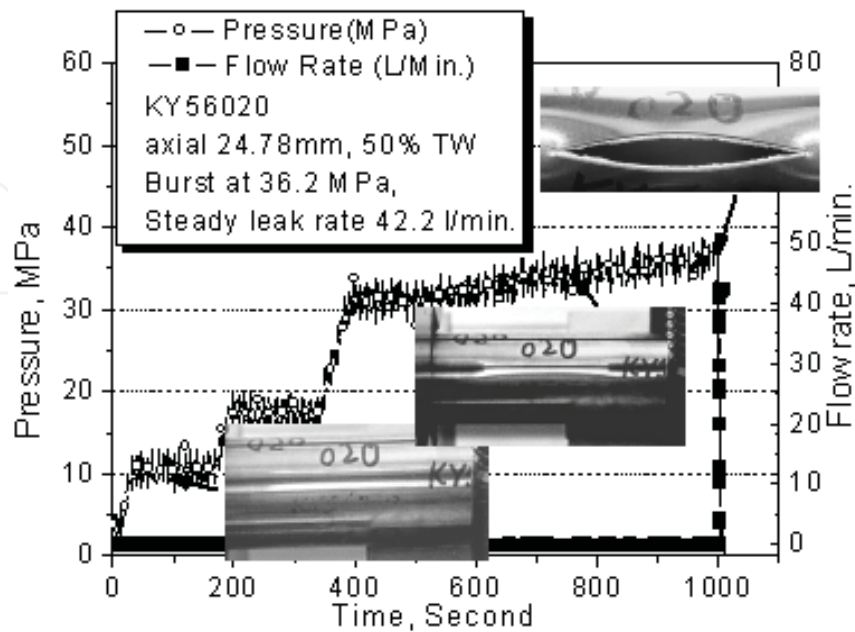


Fig. 2. Crack opening behaviour of a part through-wall flow

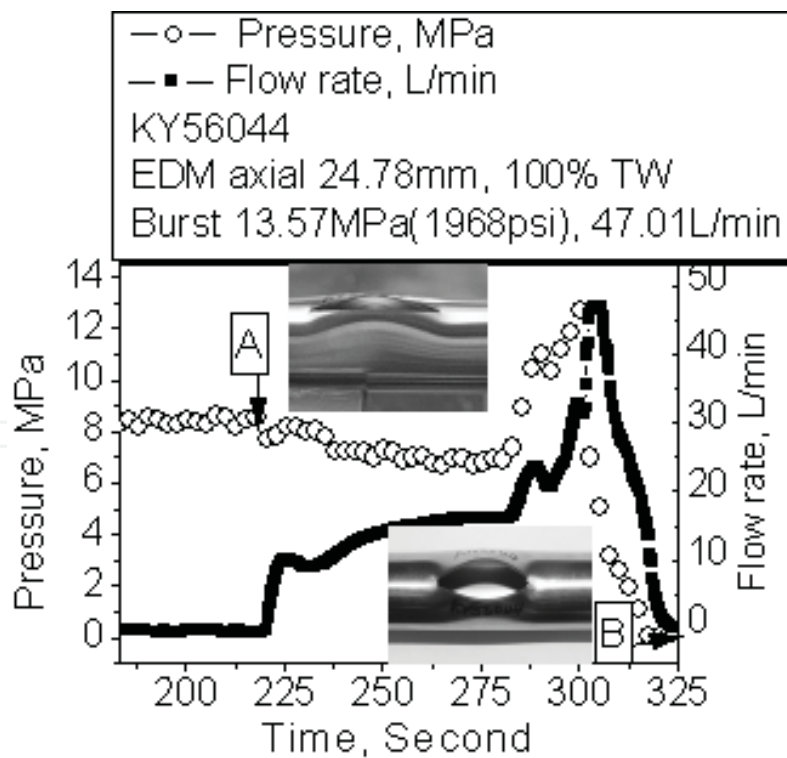


Fig. 3. Crack opening behaviour of a 100% through-wall flow

Through-wall defect tubes showed a larger COD than that of the part-through-wall defect tubes at the same pressure as shown in Fig. 3. The 175 mm long bladder inserted inside the 25 mm long 100% TW defect tube (KY56044) was perforated at 4.5 MPa, a water jet came out

of the bladder. The bladder extruded out of the defect when the pressure reached at 8.5 MPa. A hole in the bladder was enlarged at a constant pressure, and then the COD of the tube increased for 2 to 3 seconds. There was an extrusion of the bladder throughout the tube opening followed by a tube rupture. The opening was not evaluated quantitatively in this test.

3.2 Effect of the defect depth and length on the rupture/ burst pressure

Burst pressures as a function of the defect depth are plotted in Fig. 4. Closed symbols and open symbols are obtained in the present study and acquired from another research group (Cochet, 1991), respectively. Rupture pressures have a linear dependency with defect depth. These results suggest that the rupture pressure of the part through-wall tubes depends rather on the defect depth than on the defect length.

In the case of the 100% through-wall defects, they showed a strong length dependency from about 12 MPa for a 50 mm long defect to 45 MPa for a 7 mm long defect. Fig. 5 shows the rupture pressures as a function of the defect length. Closed symbols were obtained in the present study. Rupture pressure of 50 % TW defect and 75 % TW are around 35 MPa and 20 MPa, respectively regardless of their length from 25 mm up to 62 mm. Short defects below 25 mm, however, showed a dependency with the defect length.

3.3 Relationship between the flow rate, defect depth and defect length

Flow rates after the rupture of the part through-wall defect tubes were measured. Defect depths were 50% and 75 % of the wall thickness, and the defect lengths ranged from 25 mm to 62 mm. Regardless of the defect types, the flaws showed a similar flow rate of around 45 l/ min, which was the maximum flow capacity of the testing system as shown in Fig. 6.

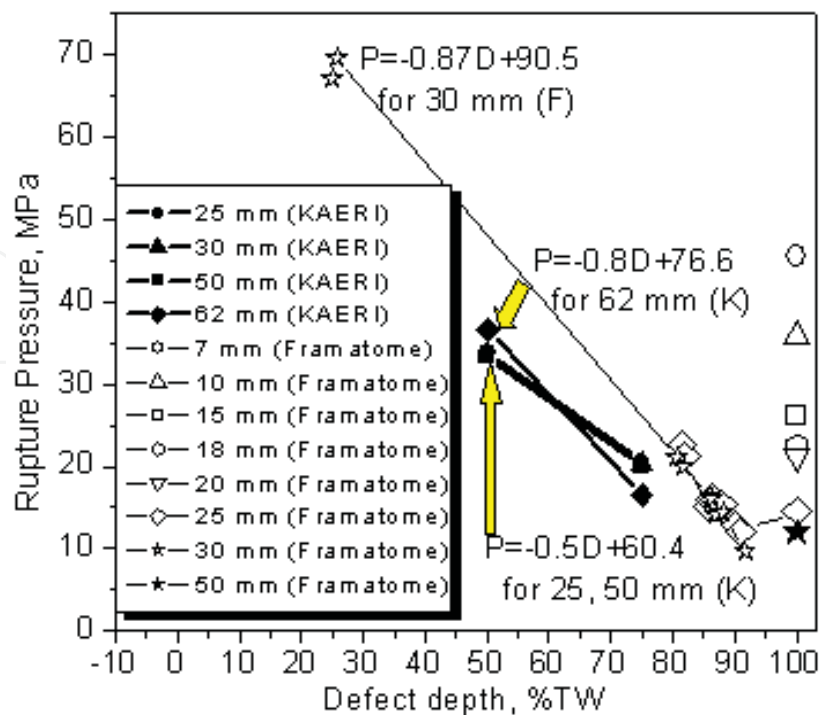


Fig. 4. Effect of the defect depth on the burst pressure

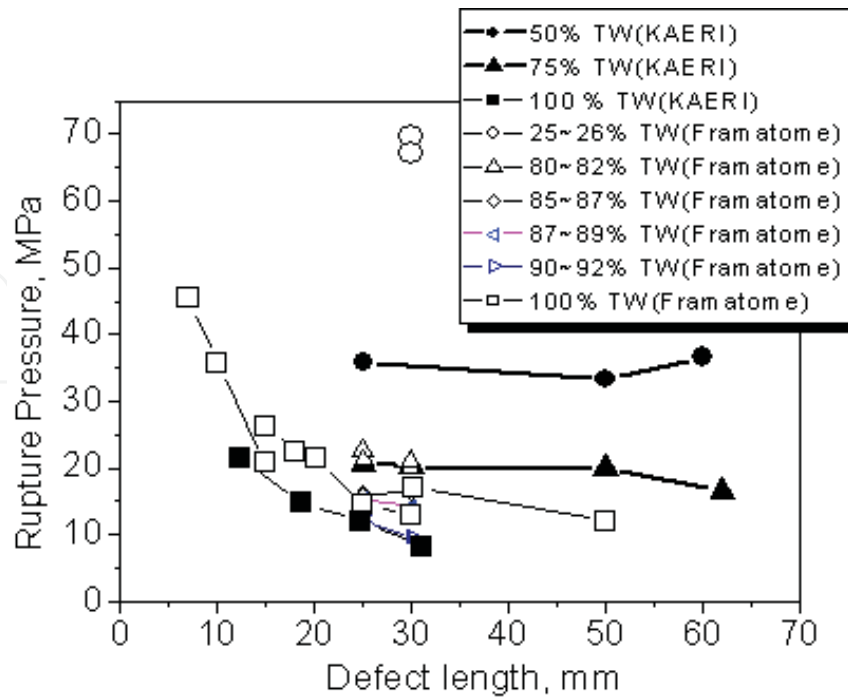


Fig. 5. Effect of the defect length on the burst pressure

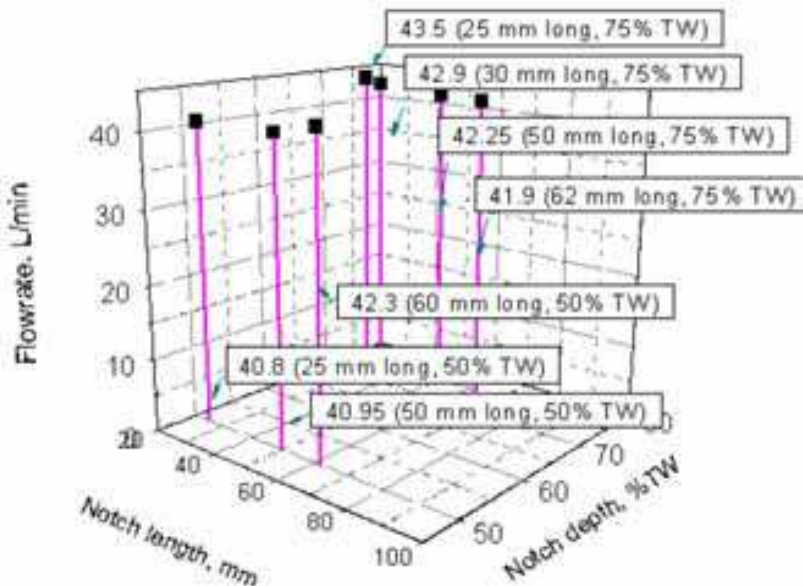


Fig. 6. Relationship among the length, depth and flow rate of the part through-wall defects

3.4 Effect of the pressurization rate on the burst pressure of a through-wall defect

A through-wall defected tube showed three stages of rupture behaviour as presented in Fig. 7; flexible plastic tube burst (stage A), the tube hole enlarged (stage B), and finally, the SG tube burst (stage C). The pressure dropped from 6 MPa to 2 MPa when the flexible plastic tube burst. When the internal water pressure increased as in stage B, the flow rate increased. The tube burst occurred at about 9 MPa.

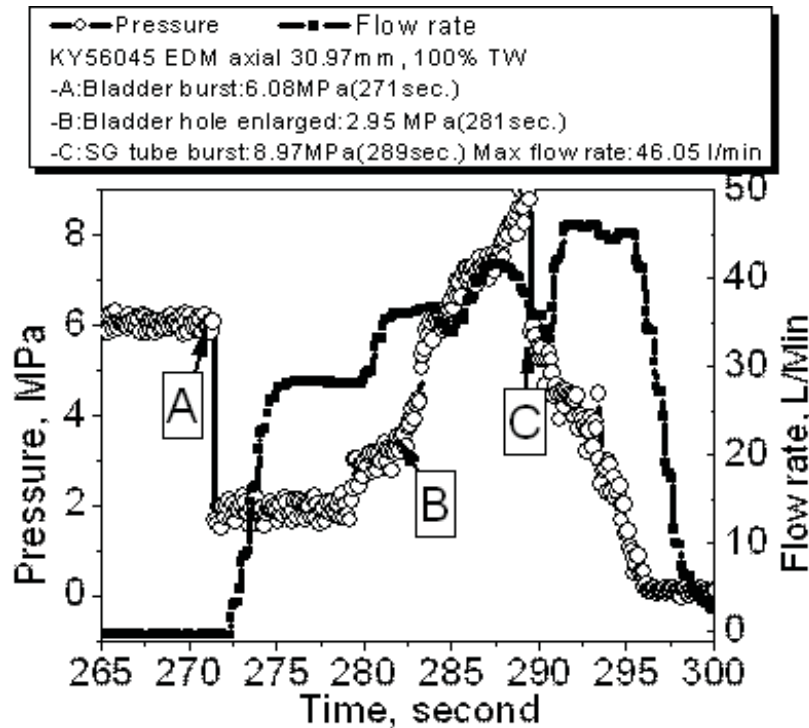


Fig. 7. Burst behaviour of a through-wall defect tube in a slow pressurization

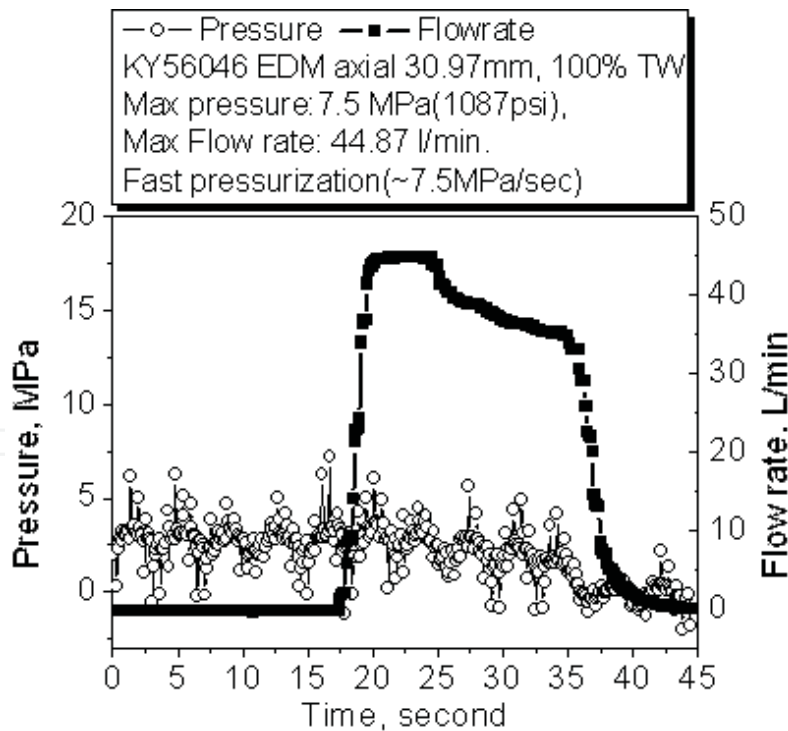


Fig. 8. Burst behaviour of the through-wall defect in a fast pressurization

Fast pressurization led to a different burst behaviour as shown in Fig. 8. The pressurization rate was about 7.5 MPa/ sec (1087 psi/ second). A pressure fluctuation between 3 MPa and 7 MPa was recorded. Maximum flow rate was achieved 2 seconds after the tube burst. Burst pressure of the tube was about 7.5 MPa, which is smaller than that of a slow pressurization

(9 MPa). It has been reported that there was no burst pressure difference between fast and slow tests without a foil (Keating, 2001). It has also been reported that if a foil reinforcement was used in the fast tests, an average burst pressure increased would be about 25 %. In case of the part through-wall defects, the ligament rupture pressure was reported to increase when the pressurization rate increased (Kasza, 2002). In this test, however, the two tubes were not equipped with a foil. It is considered that the reinforcement effect of the foil was not shown, the tube with the slow pressurization showed a high burst pressure due to the toughness of the bladder itself.

Failure morphologies after the burst of the through-wall defect with a bladder in the two pressurization modes are shown in Fig. 9. The flexible plastic tube extruded out of the SG tube after the burst in the slow pressurization mode, while the plastic tube was torn like a fish mouth in the high pressurization mode. The SG tube failure morphologies, however, are similar. This explains that the flow rates after the SG tube burst are similar at about 45 l/ min.

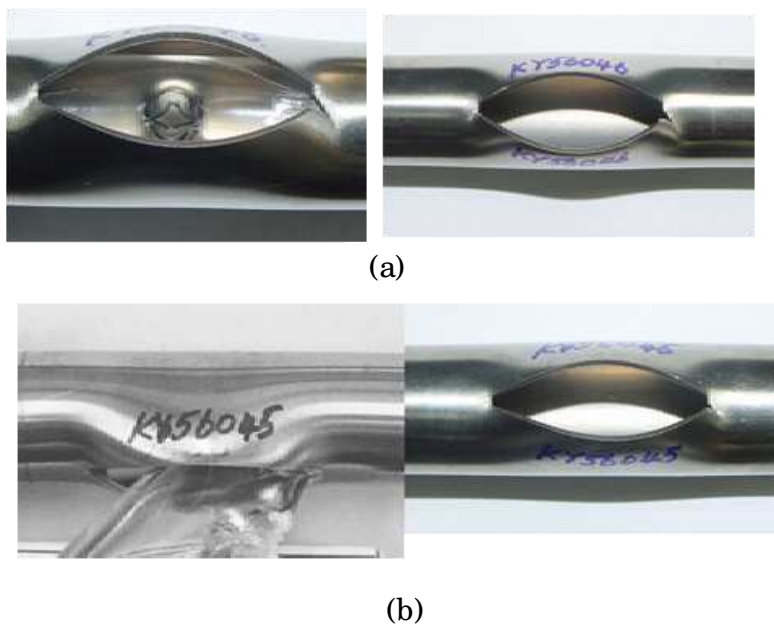


Fig. 9. (a) Fast Pressurization: Fish mouth like failure of the bladder: Burst at 7.5 MPa
(b) Slow Pressurization: Squeezed out of the bladder Burst at 8.9 MPa

3.5 Room temperature pressure test

The first leak was detected at 17.2 and 24.3 MPa for specimens SGH002 and SGH006, respectively. These pressures are similar to those used in the cracking procedure, 20.7 MPa at which it was confirmed that the tube contained a 100 % through wall crack produced by SCC under nitrogen gas pressure. A droplet was formed on specimen SGH002 at 17.2MPa, but it did not grow any more during a 5 minute hold at that pressure. At 22.0 MPa, the leak rate increased to one drop every 3 seconds. The leak rate was 0.24 l/ min at 29.6 MPa and 4.28 liter/ min at 34.5 MPa, and the specimen ruptured at 35.9 MPa. Fig. 10 shows the crack of SGH002 after the pressure and leak test done at room temperature. The crack was torn like a fish mouth, which was formed during the rupture at 35.9 MPa, and the length was about 11 mm.

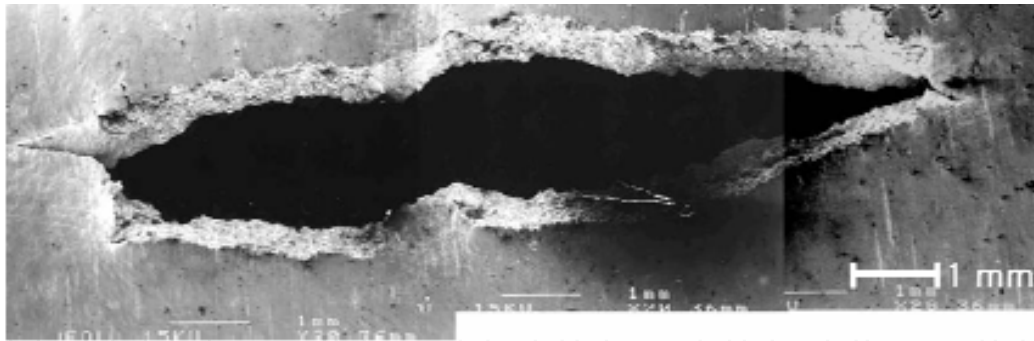


Fig. 10. Crack morphology of SGH002 taken by SEM after the pressure/ leak test at room temperature

Specimen SGH006 developed a water spray at 23.4 MPa, which subsequently decreased to a droplet flow with a drop occurring every 4 seconds. It showed a leak rate of 0.27 l/ min at 27.6 MPa and 3.87 l/ min at 34.5 MPa and ruptured at 39.3 MPa. This tube did not show a leakage at 10.8 MPa and 17.2 MPa.

The pressure test results are summarized in Table 3. Though both tubes had a 100 % through wall penetration, they did not leak at the operating pressure of 10.8 MPa. So, throughwall cracking is not a sufficient criterion for a detectable leakage. On the contrary, the crack opening or tightness is more important for showing a certain amount of the leak rate.

Tube ID	Cursory ECT(Effective crack length, mm)	Leak test RT(4) or 282°C	Leak @10.8 MPa(5)	First leak, MPa	Spray starts MPa	Leak rate 1, l/min	Leak rate 2, l/min	Burst pressure or final leak rate MPa
SGH001	OD, 95% ϕ 5.08mm, 90% ϕ 11.43mm	RT	No leak	one drop/6sec @25.0	27.4	0.19 @31.7	0.25 @31.7	-
SGH002	Axial indication(3)(10.5mm)	RT	No leak	one drop @17.2	28.3	0.24 @29.7	4.28 @34.5	35.9
SGH005	Before pressurized:100% ϕ 12.7mm After pressurized: 90% ϕ 15.24mm	282 °C	No leak	18.6	Leak @18.6, but disappeared after 15 min. No more leak @ 19.0			
SGH005 (1)	After Heat tinting (600°C 4 hrs.)(Before RT pressure test) : 100% ϕ 15.24mm	RT	Spray @ 0.41 MPa	-	0.23 l/min @10.8	0.32 @17.2	0.34 @19.0	0.43 @20.7
SGH005 (2)	"	RT	Pressurization at 6.9MPa/sec, Leak rate of 44.28 l/min at peak pressure of 34.5 MPa					
SGH006	Axial indication(3)(12.3mm)	RT	No leak	one drop @23.4	23.4	0.27 @27.6	3.87 @34.5	39.3
SGH009	Axial OD, 80% ϕ TW/10.16 mm	RT	No leak	one drop @20.7	21.8	0.019 @24.1	0.023 @24.1	0.023 @24.1(7)
SGH010	Axial OD, 85% ϕ TW/5.08mm	RT	No leak	one drop @22.8	24.8(6)	0.13 @29.7	0.16 @29.7	0.16 @30.0(7)
SGH012	Axial ID, 100% ϕ TW/24mm	282 °C	No leak					
"	"	RT	-	-	atomized spray@8.3	0.020 @8.3	6.99 @28.3	-

Material: Alloy 600 HTMA->Sensitized for 48 hours @ 600 °C

(1) Room temperature pressure test with same tube used at 282 °C(without bladder), (2) Unstable Burst test (with bladder)

(3) Not quantified, (4) RT:Room temperature, (5) Normal operating pressure difference in a PWR

(6) one drop/5 sec, one drop/9sec @ 22.8 MPa, no more drop for 1 min @24.1 MPa, and then one drop/7sec @24.1 MPa, one drop/one sec @24.

(7) 10 min interval between the measurements.

Table 3. History of the pressure test for archive tubes

In the second stage of the test, specimens SGH001, SGH009, and SGH010 did not leak at 10.8 MPa, which is the nominal normal operating pressure difference, even after a 5 minute hold time. The first leak pressures of the specimens SGH001, SGH009, and SGH010 were 25.0, 20.7, 22.8 MPa respectively, even though these tubes showed a nitrogen gas leak at 20.7 MPa during crack development. The first leaks were in the form of a single water drop forming every 4 to 8 seconds. The droplet changed into a water jet after the pressure was increased by an additional 2.4 MPa. Leak rates were measurable above the pressure at which an actual jet formed. The initial leak rates for each specimen were 0.19 l/ min at 31.7 MPa for SGH001, 0.019 l/ min at 24.1 MPa for SGH009, and 0.13 l/ min at 29.7 MPa for SGH010. For all three tubes, the leak rates increased with time due to an increase in the crack opening areas at a high pressure, but then they reached a constant leak rate after about 30 minutes.

Fig. 11 shows specimen SGH001 after the pressure test at room temperature. Two or more cracks are linked with each other along the axial direction, and they showed different opening areas.

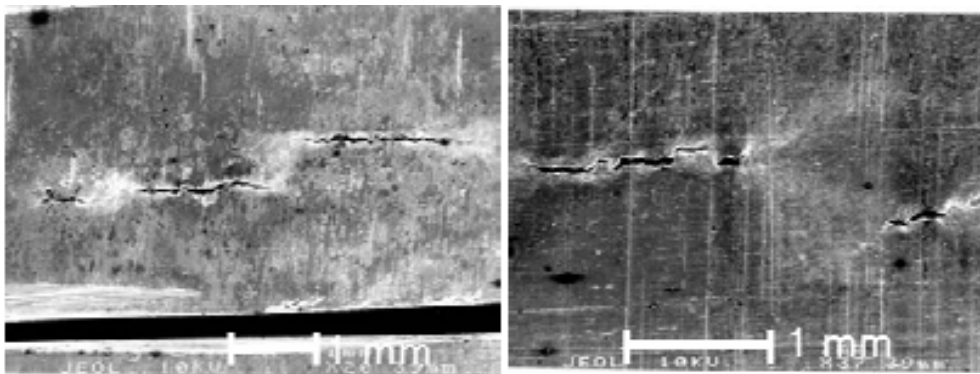


Fig. 11. Flaws on SGH001 after the pressure/ leak test at room temperature

Crack length on the inside of the tube is shorter than that on the outside of the tube. It is considered to arise from two factors; one of them is the inside pressurization procedure and the other is the crack development procedure in which the crack is initiated on the outer surface. The effective crack length, which controls the leak rate, is considered as the shorter length on the inner surface. The relationship between the leak rate and crack length is shown in Fig. 12.

The room temperature pressure test for tube SGH005 was carried out after the high temperature pressure test, which is described later in this section. The tube demonstrated a non-measurable leak in the high temperature pressure test. After the high temperature pressure test, where a non-measurable leak was detected, the specimen was heat tinted at 600 °C for 4 hours to simplify the metallography.

The crack seemed to open during the heat tinting, and showed a jet spray at 0.4 MPa, a leak rate of 0.23 l/ min at 10.8 MPa and 0.43 l/ min at 20.7 MPa. Fig. 13-(b) shows the crack after the room temperature pressure test, the length of the flaw increased a little, but other features such as crack opening do not appear to be very different from that in Fig. 13-(a), which was obtained after the high temperature pressure test. In order to determine the unstable burst pressure of the flaw, SGH005 was pressurized with a pressurization rate of 6.9 MPa/ second. Leak rate was 44.28 l/ min at the peak pressure of 34.5 MPa. There was no big change in the flaw length even after the unstable burst, whereas the crack opening increased.

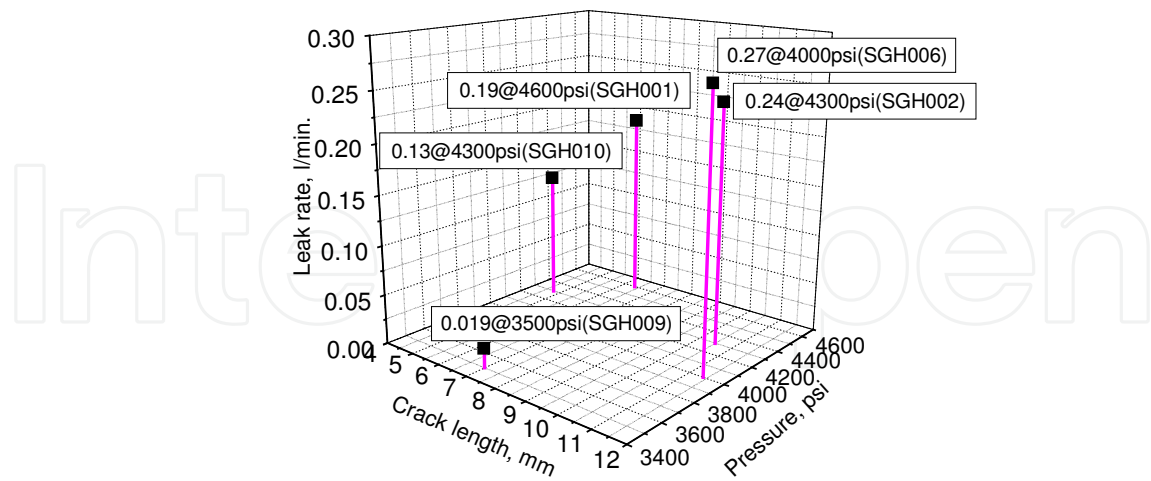


Fig. 12. Relationship between the crack length, pressure and leak rate (1000 psi = 6.9 MPa)

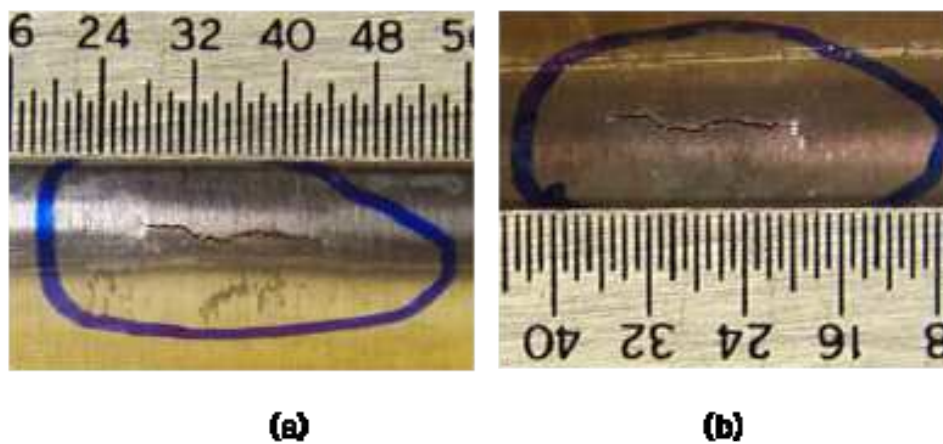


Fig. 13. Flaws on SGH005 after (a) High temperature pressure test, (b) Room temperature pressure test

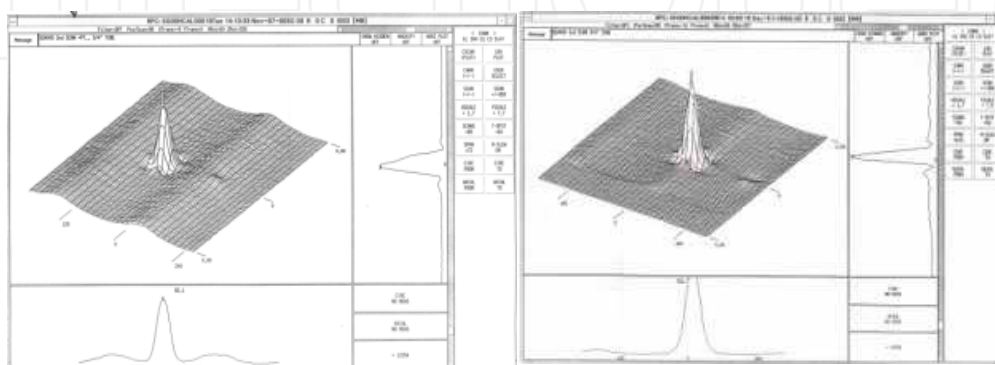


Fig. 14. Eddy current examination for SGH005, (a) before HT pressure test, (b) after HT pressure test

3.6 High temperature pressure test

Specimen SGH005, which had been confirmed as a 100 % through wall crack during the crack development, was subjected to the high temperature pressure test first. The tube did not show a leak until the pressure was 18.6 MPa. At the internal pressure of 18.6 MPa, steam was detected at the end of the muffler of the test facility. The leak rate was considered to be as low as 0.1 l/min. The leak, however, stopped after 55 minutes; no further steam was detected even after the pressure increased to the maximum value possible of 19.0 MPa in the facility. After holding it at the maximum pressure for about 10 minutes, the test was stopped and the specimen was cooled down for further testing by using the room temperature test facility.

This behaviour may be interpreted as due to a crack closure effect inside the tube while opening up the outer crack by the internal pressure. ECT (Eddy current test) indicated that the effective length of the crack after the pressure test decreased to 12.7 mm from 15.2 mm, whereas, the EC voltage increased to 99 volts after the pressure test from 30 volts before the pressure test as shown in Fig. 14. These ECT results suggest that a crack closure could have occurred during the pressurizing. However, the ECT results and the leak behaviour could be fortuitous.

SGH 012, which had an inside crack of 23 mm long, showed a similar behaviour at 282 °C. It did not show a leakage at 17.2 MPa for 135 minutes. But it showed a water spray at 8.3 MPa during the room temperature leak test.

3.7 Leak rate prediction

This work analyzed three specimens, SGH001, SGH009 and SGH010, which were pressurized to different levels and then the stable leak rates were measured before the final unstable burst.

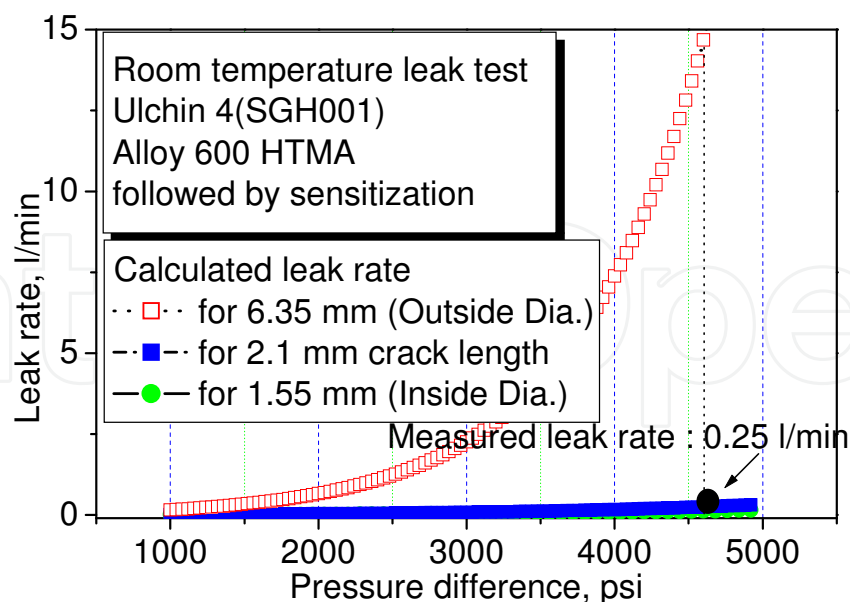


Fig. 15. Comparison of the calculated and measured leak rate for the tube SGH001 (1000 psi = 6.9 MPa)

Four different pressures were applied to obtain the leak rate from SGH001. The first leak from the tube was recorded at 25.0 MPa in the form of a single water droplet. A leak rate of

that kind of drop is considered as less than 0.01 l/min, the calculated crack length based on the leak rate model described in section 2.3 was about 0.6 mm. A measurable leak rate was obtained at 31.7 MPa, it changed a little with time at that pressure. According to the leak rate model, the calculated crack length was 2.10 mm for the final leak rate of 0.25 l/min as shown in Fig. 15. Crack lengths of the main crack of this tube were 3.85 mm and 1.55 mm outside and inside respectively. The calculated crack length of 2.1 mm was between the measured inside diameter crack length and the outside diameter. From the difference of the crack lengths between the measured and calculated one, it is considered that some of the final leak rate came from the minor cracks. The calculated crack length is also based on a simple rectangular model of the crack shape. The opening of the crack is clearly not going to be as constrained as it would be for a 1.55 mm long rectangular crack. When the pressure reached 31.7 MPa, the calculated leak rate for the 1.55 mm crack was 0.12 l/min. The measured value of 0.25 l/min is close to the calculated value for the 2.10 mm crack.

In the case of SGH009, a leak rate of 0.023 l/min was obtained at 24.1 MPa. The calculated crack length was 1.0 mm, which is longer than the inside crack length and much shorter than the OD crack length. The measured leak rate of 0.023 l/min is for the leak rate line for the 1.0 mm crack length as shown in Fig. 16. This means that the effective length of the flaw in SGH009 is also between the measured inside and outside diameter crack lengths.

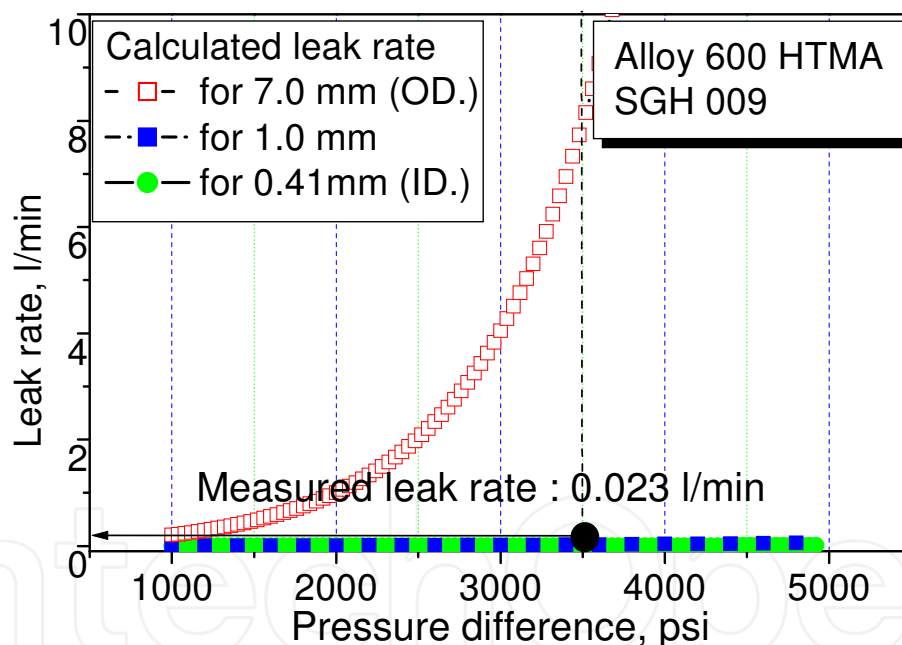


Fig. 16. Comparison of the calculated and measured leak rate for the tube SGH009 (1000 psi = 6.9 MPa)

Fig. 17 shows the relationship between the leak rate and the effective crack length of tube SGH010. Like tube SGH001, this tube showed a time dependent increase of the leak rate. Final leak rate was 0.16 l/min at 29.6 MPa, and this corresponds to an effective crack length of 1.9 mm. The calculated crack length was longer than the measured inside diameter crack length of 1.07 mm. Unlike tube SGH001, both tubes had effective crack lengths significantly greater than the limiting inner diameter length. This may be due to the larger ratio of the outer to inner diameter crack length, which leads to a lessened constraint on the crack opening.

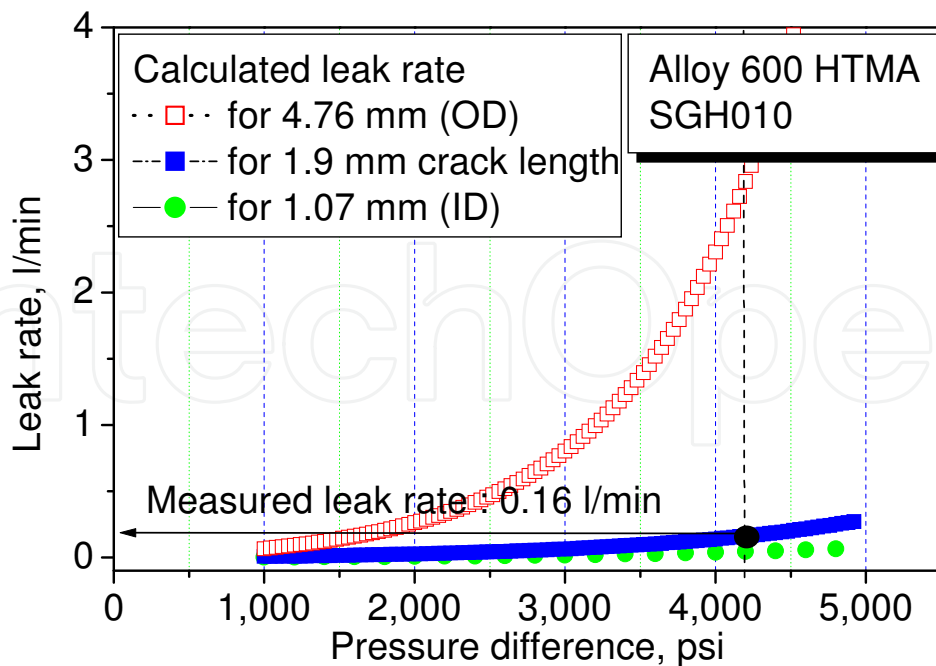


Fig. 17. Comparison of the calculated and measured leak rate for the tube SGH010

3.8 Time dependent leak rate evolution of SCC cracks

The measured leak rates were compared with those of the estimated ones based on the leak rate model developed by Argonne National Laboratory (Majumdar 2000). The SCC flaws have a characteristically different flow path through crack surface and showed a different leak behaviour from that of mechanically machined flaws. Several SG tube specimens with various SCCs were tested for the present investigation (Table 4).

Specimen No.	Flaw ID	Flaw type	COA [mm ²]	Length [mm]
KY56066	flaw-1	Axial	0.059	3.51
	flaw-2	"	0.038	3.766
	flaw-3	"	2.073	11.1
KY56068	flaw-1	"	0.648	15.04
	flaw-2	"	0.282	7.29
KY56069	flaw-1	Circumferential	0.069	8.586
	flaw-2	"	0.23	7.269
	flaw-3	"	0.027	4.13
KY56070	flaw-1	"	0.123	6.97
	flaw-2	"	0.082	6.02

Table 4. Feature of the cracks developed on the SG tubes

Fig. 18 shows the typical behaviour of the pressure and leakage rate during a water pressurization on a degraded SCC tube. In the case of the KY56065 specimen, the main crack opened at 42 MPa and a leakage began to be recorded. As the pressure increased, the crack opening area also increased. It was considerably torn at 48 MPa, and the water pressure decreased while the flow rate increased. A further increase of the water pressure at the test

time of 670 seconds enabled the crack to open further. Consequently, the leak rate rapidly increased.

Fig. 19 shows the crack features after the burst test. An initial leakage came from the circumferential cracks and a following leakage was originated from the axial ones. This is because the depth and length of the circumferential cracks are much deeper and longer than those of the axial ones respectively. On the other hand, it is also because the hoop stress is two times larger than the axial stress during a water pressurization.

The measured leak rate and an estimated one based on the leak rate model(Majumdar 2000) are shown in Fig. 20. The final measured pressure and leak rate are presented in this figure, and the photos in Fig. 19 were also obtained after a final pressurization at 31 MPa. The measured leak rate of 27.52 l/ min at 31 MPa corresponds to an equivalent crack length of 6.7 mm which is calculated from the leak rate model. Then the length of the main crack after the burst was 5 mm long, and there are multiple cracks, whose lengths were 1 mm to 5 mm as shown in Fig. 19. Since the cracks are not singular, it is hard to compare the measured crack length with the estimated one.

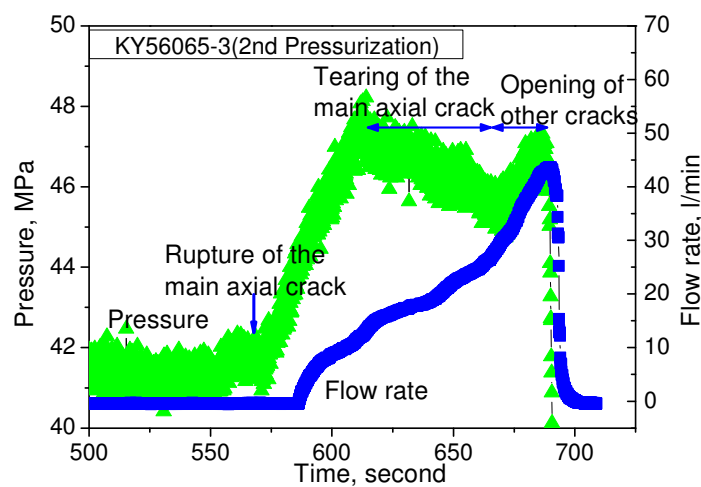


Fig. 18. Leak behaviour for a degraded SCC tube at room temperature

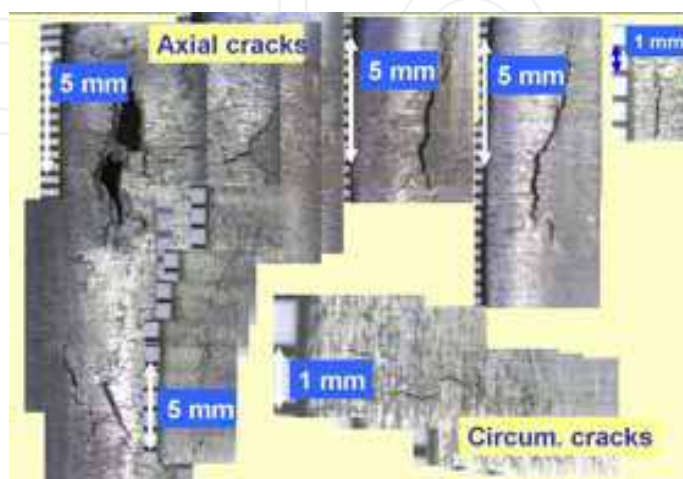


Fig. 19. Feature of the cracks after the burst test of the KY56065 specimen

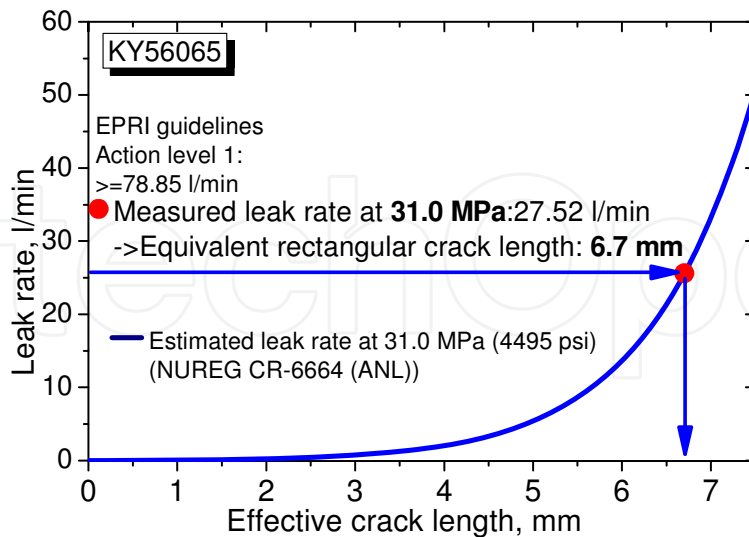


Fig. 20. Comparison on the leak rate measured and estimated based on the leak rate model

The tube showed different leak rates depending on the internal water pressure as depicted in Fig. 21. When considering a pressure difference of 8.5 MPa between the primary and secondary side of the SG tubes, the leak rate of 0.81 l/min at 26 MPa is not that big. On the other hand, the leak rate model estimates a rate of 0.32 l/min for a 6.7 mm long crack at 8.5 MPa. It can be said that multiple cracks of over 5 mm in length on a tube do not reveal the action level 1 (78.85 l/min) of the EPRI leakage guide line (EPRI, 2000).

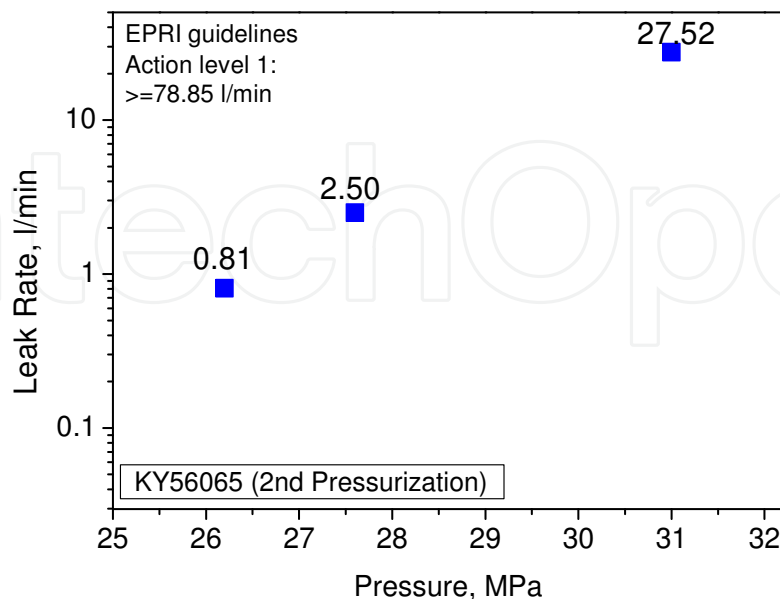


Fig. 21. Dependency of the leak rate on the pressure of a SCC degraded SG tube

The length of the cracks observed in operating steam generators is generally less than 10 mm long, as shown in Fig. 22. Based on the leak rate evaluation from the present work, these cracks might show a negligible leakage even when they are throughwall.

Leak rate from the SCC flaws at a constant pressure showed different behaviours depending on the crack tightness, crack length, or surface morphology of the cracks as shown in Fig. 23. and Fig. 24. A small increase in the leak rate was observed for one specimen (KY56069).

The specimen of KY56069 might have a tight crack, so it did not show a leak increase with the time at a constant pressure. The fact that the type of crack was circumferential seems to be another reason for the leak behaviour. The other specimen, KY56068, however, showed a distinct increase of the leak rate with the time at a constant pressure as shown in Fig. 24. As indicated in Table 4, COA (Crack Opening Area) of the KY56068 is much larger than that of KY56069. Longer crack length of KY56068 also explains the increasing leak rate with time at a constant pressure.

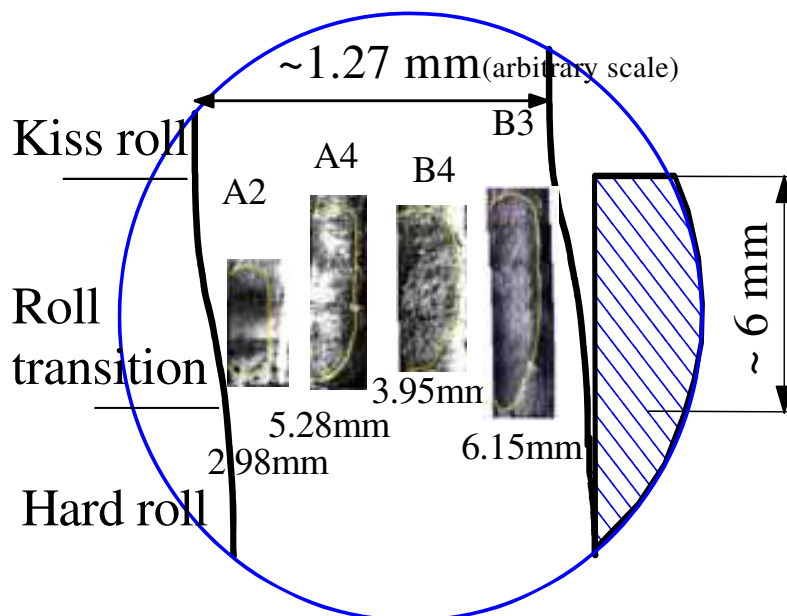


Fig. 22. Feature of the cracks from an operating steam generator

4. Conclusions

While the tube integrity was sustained before the burst, a small pressure increase of 1 MPa caused a tube ligament rupture followed by a burst. For the studied flaw length from 25 mm up to 62 mm, burst pressure of the part through-wall tubes depends rather on the defect depth than on the defect length. Flow rates after a ligament rupture of the part through-wall defect or a burst of the through-wall defect tubes were similar. Burst pressure of a through-wall defect in a fast pressurization was smaller than that of a slow pressurization.

Although all the specimens had 100% throughwall cracks developed under a pressure of 20.7 MPa, none leaked at the plant operating pressure in water. In this test, the outside crack length was at a maximum 17 times longer than the inside crack in a tube. The first leak in the form of a water droplet was detected between 17.2 MPa and 24.8 MPa depending on the flaws. Burst pressure of the through wall crack of 10 mm long was 35.9 to 39.3 MPa. Calculated leak rate for a crack length relatively close to the inside diameter crack length

(which is much smaller than the outer diameter crack length for the cracks in these tests) fits the measured leak rate well.

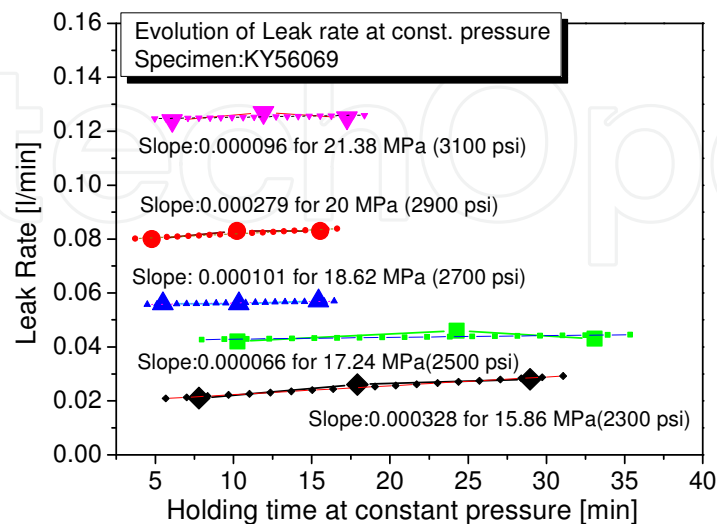


Fig. 23. Leak rate behaviour for the tight corrosion crack at a constant pressure

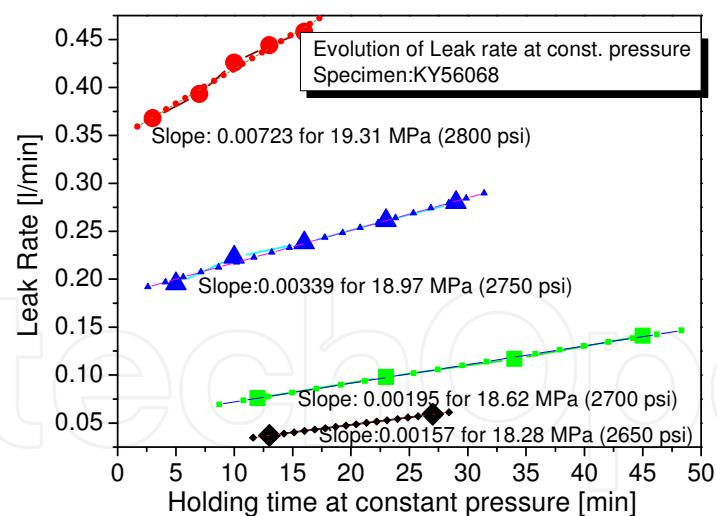


Fig. 24. Leak rate evolution for the large open crack at a constant pressure

SCC crack showed a ligament rupture at the first stage of the pressure test, then a tearing of the main crack and an opening of the crack followed. Measured leakage rate from the SCC flaws agreed reasonably with the estimated value of the leak rate model. Multiple cracks of over 5 mm in length on a tube showed a much lesser leakage rate than the EPRI leakage guidelines, action level 1 (78.85 l/min). The large open and long axial crack showed an increasing leakage rate with the time at a constant pressure.

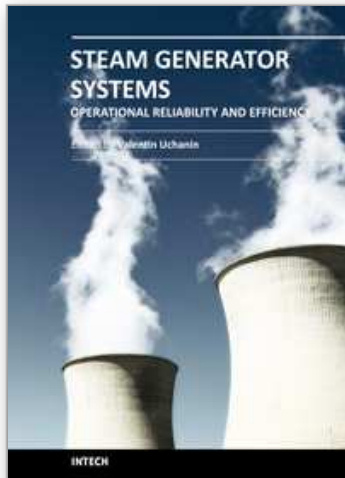
5. Acknowledgement

This work was funded by Korea Ministry of Education, Science and Technology.

6. References

- Benson, J, 1999, Steam generator progress report , EPRI TE-106365-R14.
- Cochet, B., 1991, Steam generator tube integrity, EPRI NP-6865L vol. 1.
- Diercks, D.R., Bakhtiari S., et al., 1998, Steam generator tube integrity program-annual report, NUREG/ CR-6511, Vol.2, Argonne National Laboratory.
- Diercks, D.R., Bakhtiari, S., et al., 2000, Steam generator tube integrity program-annual report, NUREG/ CR-6511, AN Vol.7, ANL-0014, Argonne National Laboratory
- Kim, JS., Hwang, S.S., et al., 1999, Destructive analysis on pulled tubes from Ulchin unit 1 Korea Atomic Energy Research Institute.
- Kim, JS, Hwang, S.S., et al., 2003, Destructive analysis on pulled tubes from Ulchin unit 4. Korea Atomic Energy Research Institute.
- MacDonald, P.E., 1996, NUREG/ CR-6365, Steam Generator Tube Failures.
- Majumdar, S., Kasza, Ken, et al., 2000, Pressure and leak rate tests and Models for failure of flawed steam generator tubes, NUREG/ CR-6664, Argonne National Laboratory.
- Zahoor, A., 1989, Ductile Fracture Handbook, Electric Power Research Institute, Palo Alto, CA.
- EPRI 104788 R2, PWR Primary To Secondary Leak Guidelines-Revision 2, Final Report, April (2000).

IntechOpen



Steam Generator Systems: Operational Reliability and Efficiency

Edited by Dr. Valentin Uchanin

ISBN 978-953-307-303-3

Hard cover, 424 pages

Publisher InTech

Published online 16, March, 2011

Published in print edition March, 2011

The book is intended for practical engineers, researchers, students and other people dealing with the reviewed problems. We hope that the presented book will be beneficial to all readers and initiate further inquiry and development with aspiration for better future. The authors from different countries all over the world (Germany, France, Italy, Japan, Slovenia, Indonesia, Belgium, Romania, Lithuania, Russia, Spain, Sweden, Korea and Ukraine) prepared chapters for this book. Such a broad geography indicates a high significance of considered subjects.

How to reference

In order to correctly reference this scholarly work, feel free to copy and paste the following:

Seong Sik Hwang, Man Kyo Jung, Hong Pyo Kim and Joung Soo Kim (2011). Burst and Leak Behaviour of SCC Degraded SG Tubes of PWRs, *Steam Generator Systems: Operational Reliability and Efficiency*, Dr. Valentin Uchanin (Ed.), ISBN: 978-953-307-303-3, InTech, Available from:
<http://www.intechopen.com/books/steam-generator-systems-operational-reliability-and-efficiency/burst-and-leak-behaviour-of-scc-degraded-sg-tubes-of-pwrs>

INTECH

open science | open minds

InTech Europe

University Campus STeP Ri
Slavka Krautzeka 83/A
51000 Rijeka, Croatia
Phone: +385 (51) 770 447
Fax: +385 (51) 686 166
www.intechopen.com

InTech China

Unit 405, Office Block, Hotel Equatorial Shanghai
No.65, Yan An Road (West), Shanghai, 200040, China
中国上海市延安西路65号上海国际贵都大饭店办公楼405单元
Phone: +86-21-62489820
Fax: +86-21-62489821

© 2011 The Author(s). Licensee IntechOpen. This chapter is distributed under the terms of the [Creative Commons Attribution-NonCommercial-ShareAlike-3.0 License](#), which permits use, distribution and reproduction for non-commercial purposes, provided the original is properly cited and derivative works building on this content are distributed under the same license.

IntechOpen

IntechOpen